ARCHIVES
of
FOUNDRY ENGINEERING

ISSN (2299-2944)
Volume 2025
Issue 2/2025

61 – 68

8/2

10.24425/afe.2025.153795

Published quarterly as the organ of the Foundry Commission of the Polish Academy of Sciences

Structure Characteristics of Si/Si-Mo Ductile Irons Solidified on a Metallic Chill

I. Stan , D.E. Anca, M. Chisamera, I. Riposan , S. Stan *
National University of Science and Technology Politehnica Bucharest, Materials Science and Engineering Faculty,
313 Splaiul Independentei, Sector 6, 060042 Bucharest, Romania,
* Corresponding author: e-mail: constantin.stan@upb.ro

Received 29.07.24; accepted in revised form 30.01.25; available online 13.06.2025

Abstract

The present work focuses on the structure characteristics of three un-inoculated ductile cast irons (0.035-0.045%Mg_{res}), at high content of Si and Mo (I. 4.55%Si/4.71%CE; II. 5.25%Si/5.05%CE; III. 4.80%Si-2.30%Mo/4.75%CE) solidified on a cast iron chill, in furan resin sand moulds. At 4.55%Si iron, there resulted a chilled zone at 6-8mm, with carbides presence, lower graphite amount, higher nodule count and ferrite amount. Si increasing up to 5.25%Si led to a limited affected surface zone (up to 3mm), characterised by no carbides and the highest nodule count. Mo addition led to the most extensive chilled zone (11-15mm), with the lowest amount of graphite and ferrite, and the highest carbides amount, at the lowest nodule count. All irons are characterised by Type V, slightly irregular spheroidal graphite morphology, typical for the Roundness Shape Factor RSF=0.62-0.75 range, at the highest position for I, intermediary for II and at the lowest position for III cast irons. A higher Graphite Nodularity (NG) level resulted when it was calculated according to ISO 16112:2017 [CGI], comparing to ISO 945-4-2019 [DI]. By the use of the Sphericity Shape Factor (with graphite real perimeter), an intermediary position of NG was obtained; it is recommended to avoid the castings rejection, due to the lower values of NG resulted from ISO 945-4-2019 stipulation for High-Si DI. The increase of Si negatively affected the nodularity, while the supplementary Mo alloying led to the lowest NG. The chill solidification appears to have less effect on the NG of 4.55%Si iron, with the maximum influence for 4.8%Si-2.3%Mo iron and by the imposed RSF=min.0.80, especially for 5.25%Si content.

Keywords: Ductile cast iron, Si/Si-Mo alloying, Nodular graphite, Metallic chill, Carbides, Ferrite, Graphite shape factors, Nodularity

1. Introduction

In the foundry industry, the solidification cooling rate of the iron castings in the mould depends on the casting parameters (mass, geometry, wall thickness), mould and cores thermal properties, melt pouring parameters etc. Internal chills could be placed inside the moulding cavity, while the external chills (high heat capacity and thermal conductivity materials) are placed on the edge of the mould cavity, in critical positions (as part of the wall of the moulding cavity), with beneficial effects on different cast alloys. The use of metallic chill to increase the local heat transfer for the cast part, to decrease the local solidification time, to remove porosities and to improve the mechanical properties, is common in the casting industry.

Chills are beneficially used for the rapid solidification of heavy casting and achievement directional solidification, which ensure controlled freezing towards the riser [1,2]. Good results were obtained by the application of the external chills to obtain a directional solidification of different alloys, such as nickel alloy composite [3], aluminium alloy [4,5] and iron castings in camshafts production [6-10]. Heavy iron castings, as ductile or grey cast irons, are of particular interest for chills applications, especially in order to control the shrinkage cavities formation [11-13] or degenerated forms of graphite, such as chunky graphite in ductile

irons. An increased solidification cooling rate based on the presence of a metal chill in the mould will change the structure characteristics parameters and properties of the iron castings, such as the thermal conductivity [14].

In Si-alloyed ductile iron castings, a very high cooling rate for permanent (metal) mould solidification affects both the graphite quality (nodule count is approximated as a linear dependency on solidification time) and the metal matrix make-up; as expected, the pearlite content decreases with increasing silicon content and increasing preheating temperature of the metal mould [15].

In previous works [16-18], it was found that the metal mould solidification of wedge casting (up to 20mm thickness) led to 30% higher nodule count (>75% at max.15μm size) and less dependency on the casting section size, at higher values of the graphite shape factors, comparing to sand mould. Metal mould led to 8-10% higher graphite nodularity, for the entire wall thickness range. The higher is the minimum imposed graphite shape factor, the lower is the graphite nodularity, for both metal and sand mould.

In conventional, un-alloyed ductile cast irons, Si content is usually up to 3wt.%. Si-alloyed ductile cast irons, also known as "High-Si Ductile Irons", contain from 3wt.%Si up to 6wt.%Si, including two important groups of materials: (a) Solid-solution strengthened ferritic spheroidal graphite cast irons (3.2-4.3wt.%Si) and (b) Oxidation and corrosion resistant ductile irons (generally 3-6wt.%Si, with or without Mo contribution, 0.2-2.0wt.%Mo).

The present work focused on the structure characteristics of three Si-alloyed, un-inoculated ductile cast irons, at high content of Si and Mo (I. 4.55%Si/4.71%CE, II. 5.25%Si/5.05%CE and III. 4.80%Si-2.30%Mo/4.75%CE) solidified on a cast iron external chill, in furan resin sand moulds.

2. Experimental Procedure

The experimental cast irons were melted in an electric induction furnace (10kg, 8000Hz, graphite crucible), with high purity pig iron, steel scrap, FeSi, FeMo and carbonic material as charge, and treated by the Tundish-cover technique (FeSiCaMgRE master alloy), without inoculation.

The "Standard Test Methods for Chill Testing of Cast Iron, ASTM A367 – 22, Test Method A, Wedge Test and Test Method B, Chill Test", are usually used to evaluate the effect of the solidification cooling rate and chill tendency of cast irons, respectively. In the present work, the test sample was designed according to the "Test Method B, Chill Test" general stipulations, but with the sample sizes adapted to the specific of a high graphitization tendency induced by high silicon content. The test samples with 6.5x21mm bases (the small one on the chill), 56mm height and 60mm length, solidified in furan resin sand moulds (20mm of sand on all sides) on a cast iron external chill (12mm thickness).

A SPECTROLAB high-end spectrometer with hybrid optic (photomultiplier tubs) and Spectroscopic Charge Coupled Device detection system detectors were simultaneously used for high precision metal analysis. The instrument achieves detection limits below 1mg/kg.

An Automatic Image Analysis (OMNIMET ENTERPRISE and analySIS® FIVE Digital Imaging Solutions software) for particles greater than 5 μm and 0.59 mm^2 as the size area of an analyzed field was used. The structure analysis [metallographic and image analysis] was recorded to evaluate ferrite (F), carbides (K) and graphite (G) amount, as well as the graphite size, count and shape forms parameters – on the sample height (3 parallel directions), up to 25mm distance from the metallic chill (1mm between the points
analysed). Graphite particles at minimum 5μm size were considered, characterised by maximum size (F_{max}), area (A_G) and convex (P_c) / real (P_r) perimeter, which were included in different shape factors (RSF/SSF) and graphite nodularity (NG) formulas, respectively.

3. Results and Discussion

The final chemical composition (4.71-5.05% carbon equivalent, hypereutectic positions) of the test cast irons is shown in Table 1. The minor elements are typical for commercial ductile irons (wt.%): 0.002-0.007Al, 0.05-0.09Cr, 0.06-0.22Ni, 0.08-0.12Cu, 0.006-0.007Ti, 0.01-0.02Sn, 0.006-0.02As, 0.005-0.013Co, 0.0015-0.0047Nb, 0.004-0.011V, 0.003-0.08W, 0.0002-0.004Pb, 0.00025Bi.

Table 1.
Chemical compositions of the Si/SiMo spheroidal graphite cast irons (wt.%)

Iron	C	Si	Mn	P	Mo	Mg	CE*
I	3.33	4.55	0.22	0.040	0.07	0.035	4.71
II	3.46	5.25	0.22	0.045	0.04	0.045	5.05
III	3.30	4.80	0.22	0.040	2.31	0.045	4.75

*CE = %C + 0.3(%Si + %P) + 0.03%Mn - 0.4%S

Figure 1 shows the representative microstructures at different distances from the metallic chill, by graphite phase (un-etching,) and metal matrix (Nital-etching), depending on the alloying grade of the test ductile cast irons.

The structure characteristics, such as the amount of graphite (Fig. 2a), ferrite (Fig.2b) and free carbides (Fig. 2c), and the nodule count (Fig. 2d) are influenced by the induced directional

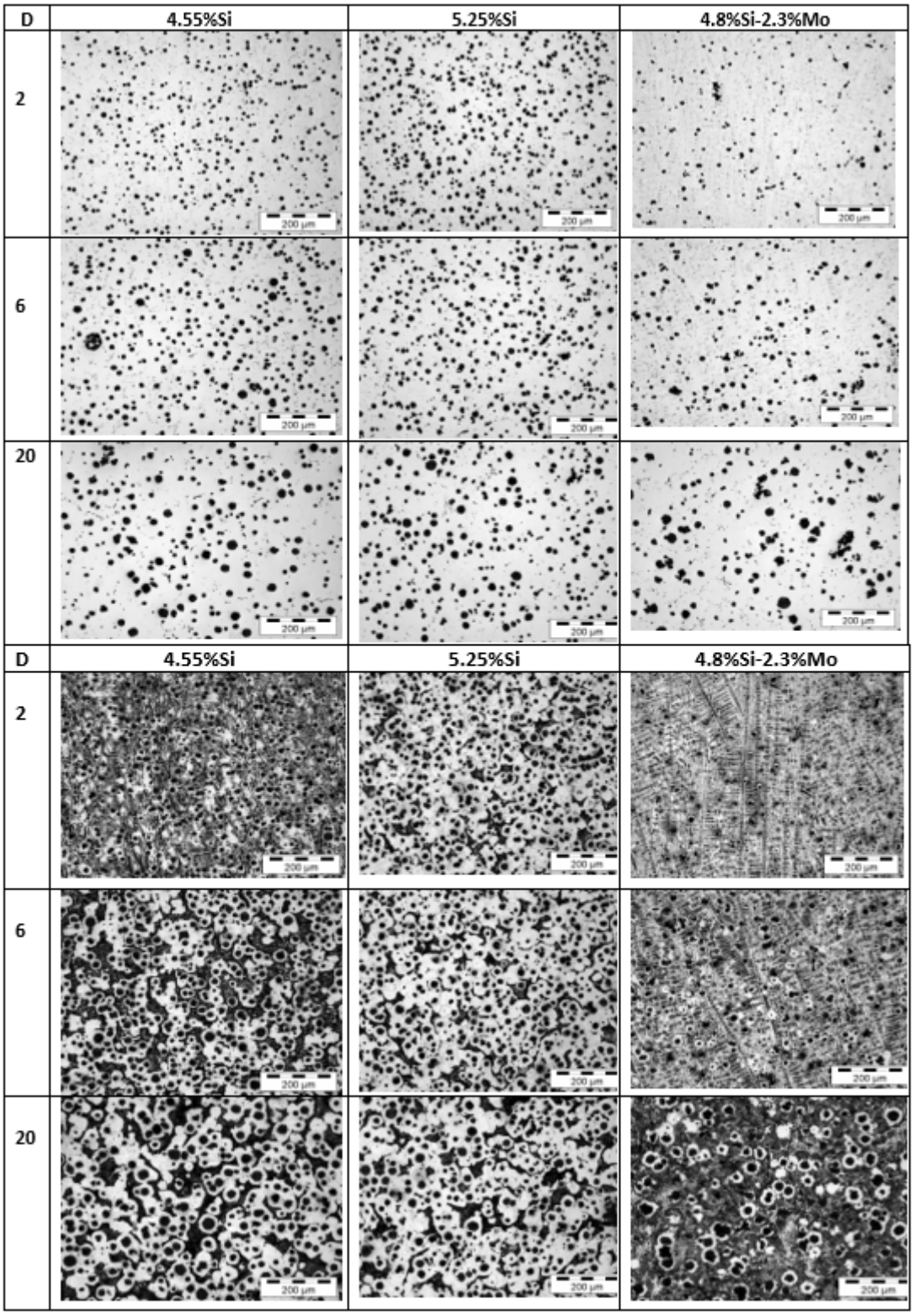

Fig. 1. Structure of Si/SiMo alloyed cast irons at different distance (D, mm) from the metallic chill (Nital etching and Un-etching)

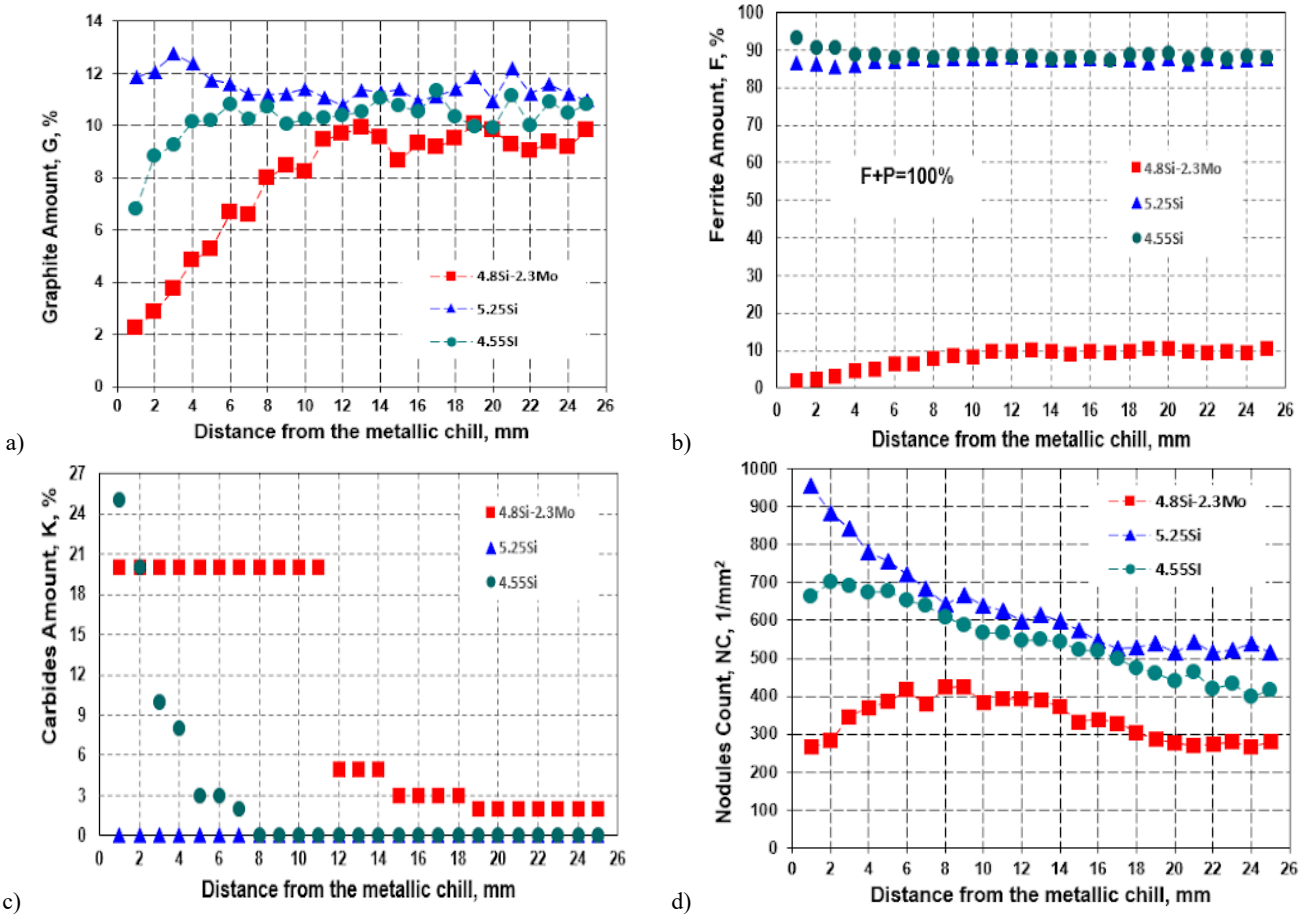

Fig. 2. The variation of the amount of graphite (a), ferrite (b) and free carbides (c) and of the nodule count (d) with the distance from the metallic chill

solidification (cooling rate decreasing from the metallic chill), the silicon level and the molybdenum addition.

The highest amount of graphite (G=10.7-12.4%) and ferrite (F=85-88%) and no free carbides presence characterise 5.25%Si alloyed iron. A metallic chill affected zone resulted, up to 3mm depth, mainly with limited graphite amount. Decreasing the silicon level to 4.55% led to visible changes, such as the structural phases amount, mainly up to 6-8mm distance from the metallic chill: lower graphite amount (with its increase from 7 to 11%), high free carbides amount (decreasing to less than 1%) and ferrite amount (decreasing from 93 to 88%). The 2.3%Mo addition to 4.8%Si cast iron strongly affected the base structure parameters, including the effects of the directional solidification: the lowest graphite amount (G=2-11%) and ferrite amount (F=2-11%) and the highest nodule count characterises 5.25%Si cast iron, with a continuous decrease from the metallic chill (from 956 to 515 Nodules/mm^2). For the lower silicon content (4.55%Si), the nodule count increases up to 2-3 mm distance from the chill (from 650 to 700 Nodules/mm^2), followed by a continuous decrease to 450 Nodules/mm^2. Si-Mo alloyed cast iron is characterised by the lowest nodule count (250-425 Nodules/mm^2), with the highest influence by the external chill solidification: increasing from 250 up to 425 Nodules/mm^2 up to 9 mm distance from the chill, followed by decreasing to the 250 Nodules/mm^2 level (Fig. 2d).

Two important graphite particles shape factors were considered, both of them involving the particle area (A_G), but differentiated by the second parameter, such as the maximum particle size (maximum Ferret-F_{max}) for Roundness Shape Factor (RSF), and the particle real perimeter (P_r) for Sphericity Shape Factor (SSF), respectively:

$$RSF=4A_G/\pi F^2_{max} \quad (1)$$

$$SSF=4\pi A_G/P_r^2 \quad (2)$$

Roundness Shape Factor is generally included in the 0.62-0.75 range (Fig. 3), which is typically for the graphite Type V (ISO), slightly irregular spheroidal graphite morphology, according to Figure 4 [19], obtained on the basis of [20, 21]. In the present experiments, the values obtained are dependant on the cast iron alloying grade: RSF=0.71-0.75 for 4.55%Si, RSF=0.68-0.71 for 5.25%Si and RSF=0.62-0.68 for 4.8%Si-2.3%Mo, respectively.

Graphite nodularity (NG) was calculated in several variants, depending on the considered graphite shape factor (RSF - Equation

1 or SSF - Equation 2), and the actual applied formulas in the International Standards referring to CGI-Compacted

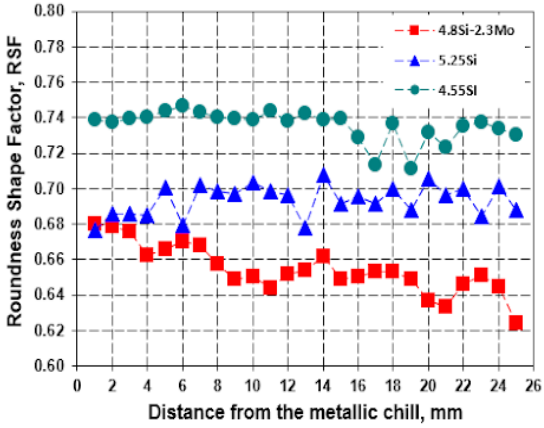

Fig. 3. Influence of the distance from the metallic chill and the cast iron alloying grade on the graphite Roundness Shape Factor-RSF

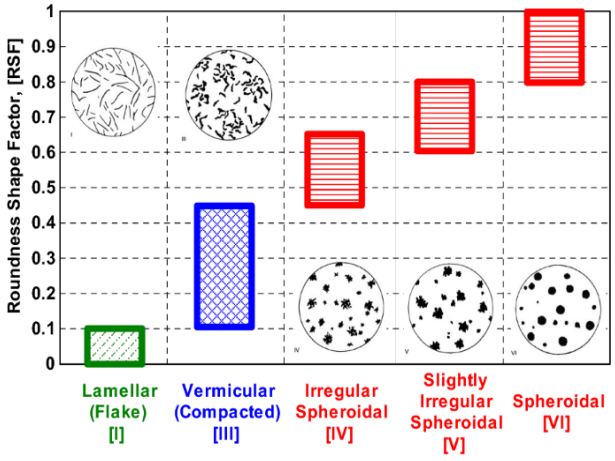

Fig. 4. Representative graphite forms (ISO 945) characterised by Roundness Shape Factor (RSF)

Graphite Cast Iron (ISO 16112:2017, CGI) [22] [NG1 - Equation 3] and to Ductile Cast Iron (ISO 945-4-2019, DI) [20] NG2 - Equation 4). Both considered standards involve the same graphite shape factor (RSF), but at different ranges and with different rate, respectively.

Replacing the Roundness Shape Factor (RSF) with the Sphericity Shape Factor (SSF) resulted in the Graphite Nodularity NG3 (Equation 5). Graphite Nodularity was also calculated by imposing a minimum accepted value for the graphite shape factor, such as for RSF, resulting NG4 (Equation 6).

$$NG1 = [(\Sigma A_{particles(RSF=0.625\text{-}1.0)} + 0.5 \cdot \Sigma A_{particles(RSF=0.525-0.625)}) / \Sigma A_{tot}] \times 100[\%] \quad (3)$$

$$NG2 = [(\Sigma A_{particles(RSF\geq 0.8)} + 0.9 \cdot \Sigma A_{particles(RSF=0.6-0.8)}) / \Sigma A_{tot}] \times 100[\%] \quad (4)$$

$$NG3 = [(\Sigma A_{particles(SSF\geq 0.8)} + 0.9 \cdot \Sigma A_{particles(SSF=0.6-0.8)}) / \Sigma A_{tot}] \times 100[\%] \quad (5)$$

$$NG4 = [\Sigma A_{particles[RSF]} / \Sigma A_{tot}] \times 100[\%] \quad (6)$$

Figure 5 shows the variation of the considered graphite nodularity NG1, NG2 and NG3 with the distance from the metallic chill, depending on the cast iron alloying grade.

Generally, the graphite nodularity is at the highest level for 4.55%Si cast iron (90-95% NG1 and 80-87% NG2), followed by 5.25%Si iron (85-90% NG1 and 65-75% NG2), with the lowest level for 4.8%Si-2.3%Mo iron (70-87% NG1 and 60-67% NG2).

If the actual standard for ductile iron is applied (ISO 945-4-2019, DI) (Equation 4), a lower value for Graphite Nodularity NG2 (60-87%) will result, as compared to mainly 85-95% NG1 based on the actual standard for compacted graphite cast iron (ISO 16112:2017, CGI) (Equation 3), showing important effects of the solidification cooling rate (distance from the metallic chill) and cast irons alloying grade, respectively.

Graphite Nodularity NG_1 is less affected by the cooling rate for both Si-alloyed cast irons, and only for a larger distance from the metallic chill (more than 17mm) it visibly decreased for SiMo cast iron.

The highest cooling rate in the metallic chill influenced zone negatively affected the graphite nodularity NG2, especially for the highest silicon content (7mm zone with 62-70% nodularity versus 70-75% for the rest of the casting).

Graphite Nodularity NG3 (Equation 5) calculated with the ISO 945-4-2019 [DI] formula, but by replacing the RSF with SSF, has an intermediary position: it is very close to NG1 for 4.55%Si, closer at 5.25%Si iron, and at a relative equidistant position for 4.8%Si-2.3%Mo iron. Generally, the curve of NG3 nodularity has the same pattern evolution as the nodularity NG1 has.

A comparison of graphite nodularity values obtained for ductile cast irons, according to the ISO 945-4-2019 stipulation formula, by the use of the graphite shape factor RSF (involving graphite particles' maximum size) [NG2] and the graphite shape factor SSF (involving graphite particles' real perimeter) [NG3] leads to visible differences. NG2 is lower than NG3 in all of the cases, and it could be a reason for iron castings quality rejection, as not respecting the imposed minimum graphite nodularity level. If, for 4.55%Si alloying grade, the graphite nodularity obtained could be accepted for both nodularity calculus formulas (NG3 = 85-95%, NG2 = 75-85%), the increase of the silicon content to 5.25% led to a larger difference (NG3 = 77-85%, NG2 = 65-75%), resulting in the possible rejection of the castings due to the lower standard graphite nodularity NG 2.

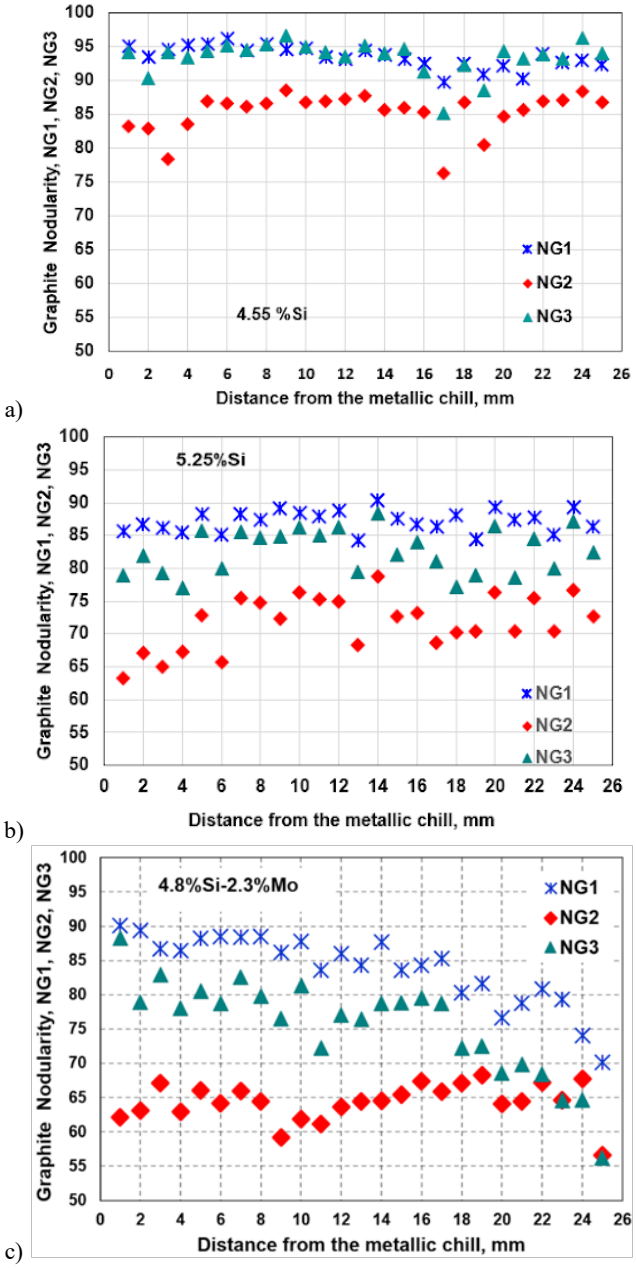

Fig. 5. Variation of the Graphite Nodularity NG1, NG2 and NG3 with the distance from the metallic chill, for 4.55%Si (a), 5,25%Si (b) and 4.8%Si-2.3%Mo (c) alloyed cast iron

The same situation occurred for 4.8%Si-2.3%Mo cast iron, with NG2 < 67% but NG3 = 70-82%. These data confirmed the previously reported results [23] that, for high-Si ductile cast irons (mainly > 4%Si), SSF (involving graphite particle real perimeter) is more representative than RSF (involving its maximum size) for the graphite nodularity calculation.

The higher the imposed minimum graphite shape factor RSF is, the lower the resulted graphite nodularity NG4 (Equation 6) is (Fig. 6), with effects of the alloying grade and solidification cooling rate: 80-98% for RSF = min. 0.50 (minimum Form IV or Intermediate Graphite) (lowest ference as alloying grade effects), 50-94% for RSF = min. 0.60-0.65 (minimum Form V) (medium difference) and 8-52% for RSF min. 0.80 (minimum Form VI) (highest difference). The increase of the Si content negatively affected NG4 nodularity, while Mo alloying led to the lowest NG4 values and the highest difference at different levels of the considered graphite shape factors.

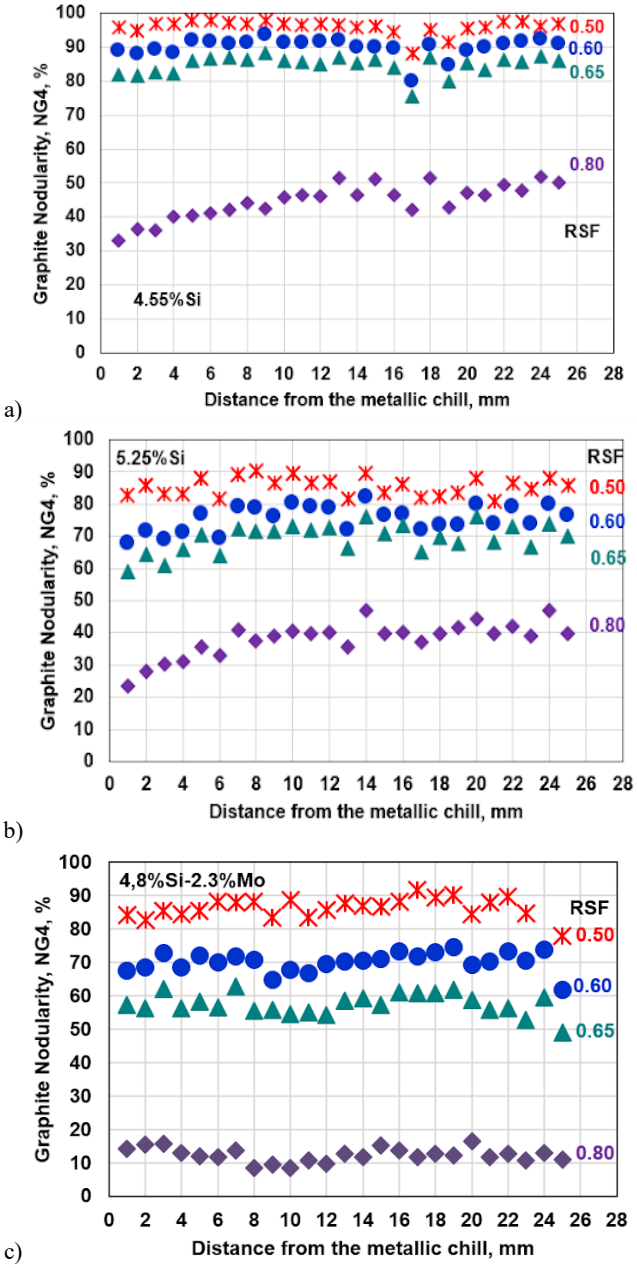

Fig. 6. Graphite Nodularity NG4 for the imposed minimum Roundness Shape Factor-RSF, at 4.55%Si (a), 5.25%Si (b) and 4.8%Si-2.3%Mo (c) ductile irons solidified on the metallic chill

If only spheroidal graphite morphologies were considered (RSF=min.0.60, see Fig. 4), such as Forms V and VI-ISO, graphite nodularity NG4 = 62-95% resulted (Fig. 7), depending on the alloying grade of cast irons: 85-95% at 4.55%Si, 70-80% at 5.25%Si and 62-75% at 4.8%Si-2,3%Mo, respectively. The same positions of different alloyed cast irons were also visible at RSF=min.0.80, as only the form VI-ISO graphite morphology was considered: less than 20% nodularity for Si-Mo alloyed iron, 20-45% at 5.25%Si and 30-50% at 4.55%Si, respectively.
The solidification cooling rate, expressed by the distance from the metallic chill, affects mainly the rate of graphite morphology Form VI-ISO in Si-alloyed cast irons, at lower level near the metallic chill (up to 8mm influencing zone), for both silicon contents.

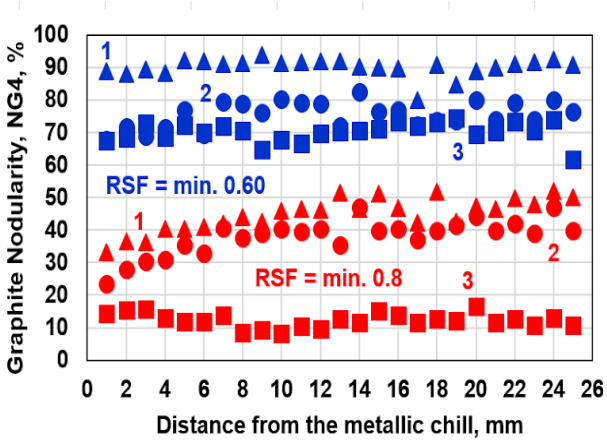

Fig. 7. Graphite Nodularity NG4 for imposed RSF=min.0.60 (V + VI forms graphite) and RSF=min.0.80 (only VI-form graphite), as effects of solidification cooling rate and cast iron alloying grade (1-4.55%Si; 2-5.25%Si; 3-4.8%Si-2.3%Mo)

4. Conclusions

The presence of a metallic chill in the resin sand mould wall led to a directional solidification of the higher silicon (4.55/5.25%Si) alloyed, uninoculated ductile cast irons, depending on the silicon content in the cast iron and supplementary molybdenum (2.3%Mo) alloying, too.

1) At 4.55%Si iron, a chilled zone of up to 6-8mm resulted, with carbides presence, lower graphite amount, higher nodule count and ferrite amount.
2) Si increasing up to 5.25%Si led to a limited affected surface zone (up to 3mm), characterised by no carbides, limited graphite amount at the highest nodule count.
3) Mo addition led to the most extensive chilled zone (11-15mm) with the lowest amount of graphite and ferrite and the highest carbides occurrence, and at the lowest nodule count.
4) All test irons are characterised by Type V-ISO, slightly irregular spheroidal graphite morphology, typical for the roundness shape factor RSF=0.6-0.8 range (involving graphite particles' maximum size), at the highest position at 4.55%Si (0.71-0.75), intermediary at 5.25%Si (0.68-0.71) and the lowest position at 4.8%Si-2.3%Mo (0.62-0.68).
5) As nodularity (NG), the test irons have positions similar to the RSF range, at higher level if it is calculated by the use of RSF according to ISO 16112:2017 [CGI-NG1], versus ISO 945-4-2019 [DI-NG2].
6) By replacing RSF with the sphericity shape factor SSF (involving graphite particles' real perimeter), intermediary positions resulted for the graphite nodularity (NG3) comparing with the actual stipulations in the two considered standards (NG2 < NG3 < NG1).
7) The previously reported results [23] are confirmed; as for high-Si DI (mainly > 4%Si), SSF is more representative than RSF therefore the graphite nodularity NG3 calculation is recommended, in order to avoid the castings rejection due to lower values of the actual stipulated NG2.
8) The higher the imposed minimum graphite shape factor is, the lower the NG is. The increasing of the Si content negatively affected the NG, while the supplementary Mo alloying led to the lowest NG.
9) The chill solidification appears to affect the NG of 4.55%Si iron less, with the maximum influence for 4.8%Si-2.3%Mo iron (NG decreasing with the distance from the chill) and by imposed RSF=min.0.80, especially at 5.25%Si content.

Acknowledgements

This work was supported by a grant from the National Program for research of the National Association of Technical Universities - GNAC ARUT 2023

References

[1] Campbell, J. (2015). *Complete Casting Handbook.* Butterworth Heinemann Publisher.
[2] Foundry: Management&Technology. (2015). *What, Why and Where for Chilling Large Molds.* Retrieved June 20, 2024, from https:///foundrymag.com/ask-the-expert/article/21928515/ what-why-and-where-for-chilling-large-molds.
[3] Purushotham, G. & Hemanth, J. (2014). Action of chills on microstructure, mechanical properties of chilled ASTM A 494 M grade Nickel alloy reinforced with fused SiO2 metal matrix composite. *Procedia Materials Science.* 5, 426-433. https://doi.org/10.1016/j.mspro.2014.07.285.
[4] Jain, S.K. & Jain, V. (2014). Effect of chill size and material on temperature gradient in aluminium alloys casting. *Journal of Material Science and Mechanical Engineering (JMSME).* 1(2), 106-112. ISSN: 2393-9109.
[5] Piekos M. & Zych, J. (2019). Investigations of the influence of the zone of chills on the casting made of AlSi7Mg alloy with various wall thicknesses. *Archives of Foundry Engineering.* 19(1), 127-132. DOI 10.24425/afe.2019.127106.
[6] Gobinath, V.M., Adarsh Kumar, Annamalai K. & Rajadurai A. (2015). Effect of pouring temperature in chilled cast iron with different chill material. *International Journal of Applied Engineering Research.* 10(57), 160-163.
[7] Kumruoglu, L.C. (2009). Mechanical and microstructure properties of chilled cast iron camshaft: experimental and

computer aided evaluation. *The Journal of Materials and Design*. 30(4), 927-938. https://doi.org/10.1016/j.matdes.2008.07.008.
[8] Yang, Y., Rosochowski, A., Wang, X. & Jiang, Y. (2004). Mechanism of "black line" formation in chilled cast iron camshafts. *Journal of Materials Processing Technology.* 145(2), 264-267. https://doi.org/10.1016/S0924-0136(03)00678-2.
[9] Ping, L., Fengjun, L., Anke, C. & Bokang, W. (2009). Fracture analysis of chilled cast iron camshaft. *China Foundry.* 6(2), 104-108.
[10] Binfeng, H (2012). Effect of Lanthanum on microstructure and properties of chilled iron camshaft. *China Foundry,* 9(1), 60-63.
[11] Vaskova, I, Conev, M. & Hrubovcakova, M. (2017). The influence of using different types of risers or chills on shrinkage production for different wall thickness for material EN-GJS-400-18LT. *Archives of Foundry Engineering.* 17(2), 131-136. DOI: 10.1515/afe-2017-0064.
[12] Hajkowski, J., Roquet, P., Khamashta, M., Codina, E. & Ignaszak, Z. (2017). Validation tests of prediction modules of shrinkage defects in cast iron sample. *Archives of Foundry Engineering.* 17(1), 57-66. DOI: 10.1515/afe-2017-0011.
[13] Yoo, S.M., Cho, Y.S., Lee, C.C., Kim, J.H., Kim, C.H. & Choi J.K. (2007). Optimization of casting conditions for heat and abrasion resistant large grey iron castings. *China Foundry.* 4(2), 124-127.
[14] Holmgren, D., Dioszegi, A. & Svensson, I.L. (2007). Effects of carbon content and solidification rate on thermal conductivity of grey cast iron. *China Foundry.* 4(3), 210-214.
[15] Riebisch, M., Seiler, C., Pustal, B. & Buhrig-Polaczek, A. (2019). Microstructure of as-cast high-silicon ductile iron produced via permanent mold casting. *International Journal of Metalcasting.* 13(1), 112-120. https://doi.org/10.1007/s40962-018-0232-5.
[16] Stan, I., Anca, D.E., Riposan, I. & Stan, S. (2023). Solidification pattern of 4.5%Si ductile iron in metal mould versus sand mould castings. *Journal of Thermal Analysis and Calorimetry.* 148, 1805-1817. https://doi.org/10.1007/s10973-022-11832-4.
[17] Anca, D.E., Stan, I., Riposan, I. & Stan, S. (2022). Graphite compactness degree and nodularity of high-si ductile iron produced via permanent mold versus sand mold casting. *Materials.* 15(8), 2712, 1-19. https://doi.org/10.3390/ma15082712.
[18] Riposan, I., Stan, S., Anca, D., Stefan, E., Stan, I. & Chisamera, M. (2023). Structure characteristics of high-Si ductile cast irons. *International Journal of Metalcasting*. 17, 2389-2412. https://doi.org/10.1007/s40962-022-00938-y.
[19] Stan, S., Riposan, I., Chisamera, M. & Stan, I. (2019). Solidification characteristics of silicon alloyed ductile cast irons. *Journal of Materials Engineering and Performance*. 28(1), 278-286. https://doi.org/10.1007/s11665-018-3828-2.
[20] ISO 945-4-2019. Microstructure of cast irons-part 4: determination of nodularity in spheroidal graphite cast irons. International Standard Organization (ISO). Geneva, Switzerland.
[21] GB/T 9441-2009. Metallographic test for evaluation of spheroidal graphite cast iron (National Standard of the People's Republic of China). Standardization Administration of China. Beijing, China.
[22] ISO 16112:2017. Compacted (vermicular) graphite cast irons-classification. International Standard Organization (ISO). Geneva, Switzerland.
[23] Riposan, I., Anca, D., Stan, I., Chisamera, M. & Stan, S. (2022). Graphite nodularity evaluation in high-Si ductile cast irons. *Materials.* 15(21) 7685, 1-14. https://doi.org/10.3390/ma15217685.